International Journal of Microwave and Wireless Technologies

cambridge.org/mrf

Research Paper

Cite this article: Gholami Mayani M, Asadi S, Karimian S (2019). Time-domain analysis of a CRLH coupled-line coupler using the CN-FDTD method. *International Journal of Microwave and Wireless Technologies* **11**, 94–103. https://doi.org/10.1017/S1759078718001393

Received: 27 June 2018
Revised: 14 September 2018
Accepted: 19 September 2018
First published online: 21 November 2018

Key words:
CN-FDTD; coupled-line coupler; metamaterials

Author for correspondence:
Shahrooz Asadi, E-mail: Sh_asadi@sbu.ac.ir

Time-domain analysis of a CRLH coupled-line coupler using the CN-FDTD method

Mahdieh Gholami Mayani, Shahrooz Asadi and Shokrollah Karimian

Electrical Engineering Department, Shahid Beheshti University, Tehran, Iran

In this study, the implicit Crank–Nicolson finite-difference time-domain (CN-FDTD) method is applied to discretize the governing telegrapher's equations of a composite right-/left-handed (CRLH) coupled-line coupler. The unconditionally stable CN-FDTD is compared with the conventional leap-frog (LF) FDTD method. The results obtained from the CN-FDTD scheme show up to 10 times increase in the temporal step size, reflecting in a dramatic decrease in processing time; in addition to having a good agreement with the LF method and the measurements.

Introduction

Due to their special properties [1–3], there has been an ever-increasing use of metamaterial-based components in the implementation of microwave devices such as couplers and filters. The metamaterial transmission line (TL) theory has been investigated by several research groups [4–7].

The pure left-handed (LH) lines demonstrating backward-wave propagation are realized by cascaded series capacitances and shunt inductances. Since the LH structures are implemented on a host line making subsequent parasitic effects (corresponding to the line inductance and capacitance), the pure LH characteristics are not feasible in practical cases. Therefore, the concept of composite right-/left-handed (CRLH) TL including both the right-handed (RH) and LH parts is introduced which shows backward-wave propagation at low frequencies and forward-wave propagation at high frequencies (the RH characteristics). The most favored planar CRLH structures can be the series interdigital capacitors and shunt shorted stubs which offer simultaneously negative ε and μ [6, 8], enabling decrease in size and potential performance improvement [9–12].

In conventional couplers, the compromise between bandwidth and coupling level has been a challenging task [13, 14]. In Lange couplers, both broad bandwidth and tight coupling can be achieved at the cost of bonding wires resulting in parasitic effects at high frequencies [15]. The CRLH couplers have also shown to provide broad bandwidth and tight coupling, and so can be used as alternatives to the conventional counterparts [11, 16]. Regarding this coupler as a multi-conductor TL (MCTL), coupled differential equations can be obtained that have no analytical solution, and so the numerical methods become very useful in such cases.

The full-wave analysis method which numerically solves the partial differential equations is rigorously accurate [17], but as a global modeling approach, it requires high CPU usage. Although, attempts have been made to decline the computational demand, it is still difficult to justify this approach in many practical cases [18–20] and this is where time-domain analysis has shown to be very efficient. The time-domain analysis of metamaterial TLs has been accomplished based on the method of moment and the Green's function method [21–23]. The finite-difference time-domain (FDTD) method as a versatile and easy-to-implement technique is successfully applied to numerical solutions. Recently, the CRLH TL has been analyzed based on the leap-frog (LF) FDTD method [7, 24]. But the LF method is conditionally stable due to the Courant–Friedrichs–Lewy (CFL) constraint [25].

On the other hand, the unconditionally stable implicit Crank–Nicolson FDTD (CN-FDTD) is similar to the LF scheme in terms of second-order accuracy in both space and time domain [26, 27]. The well-known CN-FDTD method has been efficiently applied to time-domain solution of Maxwell's equations and it has been more considerable by EM communication after 2000 [27–29]. In the CN method, selecting a larger time step size (Δt) leads to a remarkable decline in the CPU time compared with the conditionally stable methods. It should be mentioned that, the more Δt increases, the less accuracy is achieved [28, 29]; thus, Δt should be selected considerately. In general, a huge sparse irreducible matrix arising from spatial discretization is inevitable in the CN-FDTD method, though this is not considered to be a negative consequence in one dimension (1D) along x (x being the direction of propagation) such as the problem at hand.

As the CN-FDTD method, the alternating direction implicit (ADI) FDTD is unconditionally stable [30]. The CN-FDTD method has less numerical dispersion with respect to the ADI scheme [30–32]; therefore, it is expected that this method supersedes the ADI-FDTD method very soon. Concerning the huge computational cost of the CN method for general 3D problems, to date some efforts have been made. For example, the locally 1D FDTD method shows more efficiency than that of the conventional ADI-FDTD method [33–35]. It should be mentioned that two unconditionally stable methods (other than the CN scheme) have been applied to analyze the MCTLs [36, 37] and also single CRLH TL [7, 38]. Yet, the application of the CN-FDTD method to a multi-conductor CRLH TLs has not been reported. As a result, the computational time gain and guarantying the efficient analysis of CRLH MCTLs are unknown in the said cases. Although applying the CN-FDTD method decreases the computation time in 1D, this scheme suffers from a huge sparse block banded matrices in 3D problems [28].

In the present study, a CRLH coupled-line coupler is studied in 1D. The CN-FDTD method is applied to this coupler, depicted in Fig. 1(a). The constituent unit cell is shown in Fig. 2(a). In “Results and discussion” section, the results are presented in time domain and also using the scattering parameters. In order to validate the CN-FDTD scheme, the accuracy and the time gain achieved from this method are compared with those of the LF scheme and the measurement.

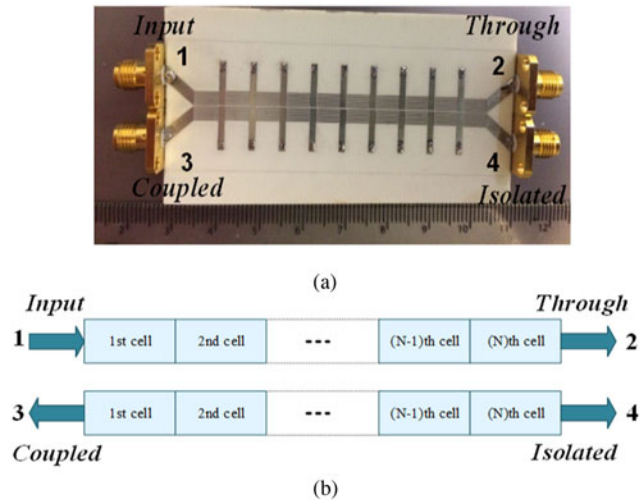

Fig. 1. (a) The fabricated coupler, (b) operational block diagram of a typical CRLH coupled-line coupler.

Mathematical approach

The block diagram of a typical CRLH coupled-line coupler consisting of two coupled CRLH TLs is depicted in Fig. 1(b) and the equivalent circuit model of one of coupled unit cells is shown in Fig. 2(b). For an infinitesimal line section with length Δx, applying the Kirchhoff's current and voltage laws to this unit cell leads to:

$$\begin{cases} \dfrac{\partial v_1}{\partial x} + R^{(1)} i_1 + L_R^{(1)} \dfrac{\partial i_1}{\partial t} + L_m \dfrac{\partial i_2}{\partial t} + \dfrac{v_{C_L^{(1)}}}{\Delta x} = 0 \\ \dfrac{C_L^{(1)}}{\Delta x} \dfrac{\partial v_{C_L^{(1)}}}{\partial t} - i_1 = 0 \\ \dfrac{\partial v_2}{\partial x} + R^{(2)} i_2 + L_m \dfrac{\partial i_1}{\partial t} + L_R^{(2)} \dfrac{\partial i_2}{\partial t} + \dfrac{v_{C_L^{(2)}}}{\Delta x} = 0 \\ \dfrac{C_L^{(2)}}{\Delta x} \dfrac{\partial v_{C_L^{(2)}}}{\partial t} - i_2 = 0 \end{cases}, \qquad (1a)$$

$$\begin{cases} \dfrac{\partial i_1}{\partial x} + G^{(1)} v_1 + C_R^{(1)} \dfrac{\partial v_1}{\partial t} - C_R^{(12)} \dfrac{\partial v_2}{\partial t} + \dfrac{i_{L_L^{(1)}}}{\Delta x} = 0 \\ \dfrac{L_L^{(1)}}{\Delta x} \dfrac{\partial i_{L_L^{(1)}}}{\partial t} - v_1 = 0 \\ \dfrac{\partial i_2}{\partial x} + G^{(2)} v_2 - C_R^{(12)} \dfrac{\partial v_1}{\partial t} + C_R^{(2)} \dfrac{\partial v_2}{\partial t} + \dfrac{i_{L_L^{(2)}}}{\Delta x} = 0 \\ \dfrac{L_L^{(2)}}{\Delta x} \dfrac{\partial i_{L_L^{(2)}}}{\partial t} - v_2 = 0 \end{cases}, \qquad (1b)$$

where $R^{(p)}$, $G^{(p)}$, $C_R^{(p)}$, $L_R^{(p)}$ correspond to the per-unit-length resistance, conductance, capacitance, and inductance parameters, respectively, and $C_L^{(p)}$, $L_L^{(p)}$ are the times-unit-length parameters in the CRLH TL. The superscript p is associated with the designated number for the lines. Also, v_1, i_1 and v_2, i_2 represent the voltages and currents, respectively, along the first and second coupled lines and $v_{C_L^{(p)}}$ refers to the voltage along C_L and $i_{L_L^{(p)}}$ is the current flowing into the L_L. These equations are considered with initial value of zero for current and voltage, giving:

$$\begin{cases} C_R^{(11)} = C_R^{(1)} + C_m \\ C_R^{(22)} = C_R^{(2)} + C_m \\ C_R^{(12)} = C_m \end{cases}, \qquad (2)$$

where in the C_m represents the mutual coupling capacitance between the coupled unit cells. The above equations can be written in a matrix form:

$$\begin{cases} \mathbf{v}_x + \mathbf{R} \cdot \mathbf{i} + \mathbf{L}_R \cdot \mathbf{i}_t + \dfrac{\mathbf{v}_{C_L}}{\Delta x} = 0 \\ \dfrac{\mathbf{C}_L}{\Delta x} \cdot (\mathbf{v}_{C_L})_t - \mathbf{i} = 0 \end{cases} \qquad (3)$$

and

$$\begin{cases} \mathbf{i}_x + \mathbf{G} \cdot \mathbf{v} + \mathbf{C}_R \cdot \mathbf{v}_t + \dfrac{\mathbf{i}_{L_L}}{\Delta x} = 0 \\ \dfrac{\mathbf{L}_L}{\Delta x} \cdot (\mathbf{i}_{L_L})_t - \mathbf{v} = 0 \end{cases}, \qquad (4)$$

where in

$$\begin{aligned} &\mathbf{v} = [v_1 \quad v_2]^T, \ \mathbf{v}_{C_L} = [v_{C_L^{(1)}} \quad v_{C_L^{(2)}}]^T, \\ &\mathbf{i} = [i_1 \quad i_2]^T, \ \mathbf{i}_{L_L} = [i_{L_L^{(1)}} \quad i_{L_L^{(2)}}]^T, \\ &\mathbf{R} = \begin{bmatrix} R^{(1)} & 0 \\ 0 & R^{(2)} \end{bmatrix}, \ \mathbf{G} = \begin{bmatrix} G^{(1)} & 0 \\ 0 & G^{(2)} \end{bmatrix}, \\ &\mathbf{L}_R = \begin{bmatrix} L_R^{(1)} & L_m \\ L_m & L_R^{(2)} \end{bmatrix}, \ \mathbf{C}_R = \begin{bmatrix} C_R^{(11)} & -C_R^{(12)} \\ -C_R^{(12)} & C_R^{(22)} \end{bmatrix}, \\ &\mathbf{L}_L = \begin{bmatrix} L_L^{(1)} & 0 \\ 0 & L_L^{(2)} \end{bmatrix}, \ \mathbf{C}_L = \begin{bmatrix} C_L^{(1)} & 0 \\ 0 & C_L^{(2)} \end{bmatrix}. \end{aligned} \qquad (5)$$

Evidently, in the general case, since there is no analytical solution to these equations, numerical methods are worthwhile to tackle the problem.

https://doi.org/10.1017/S1759078718001393 Published online by Cambridge University Press

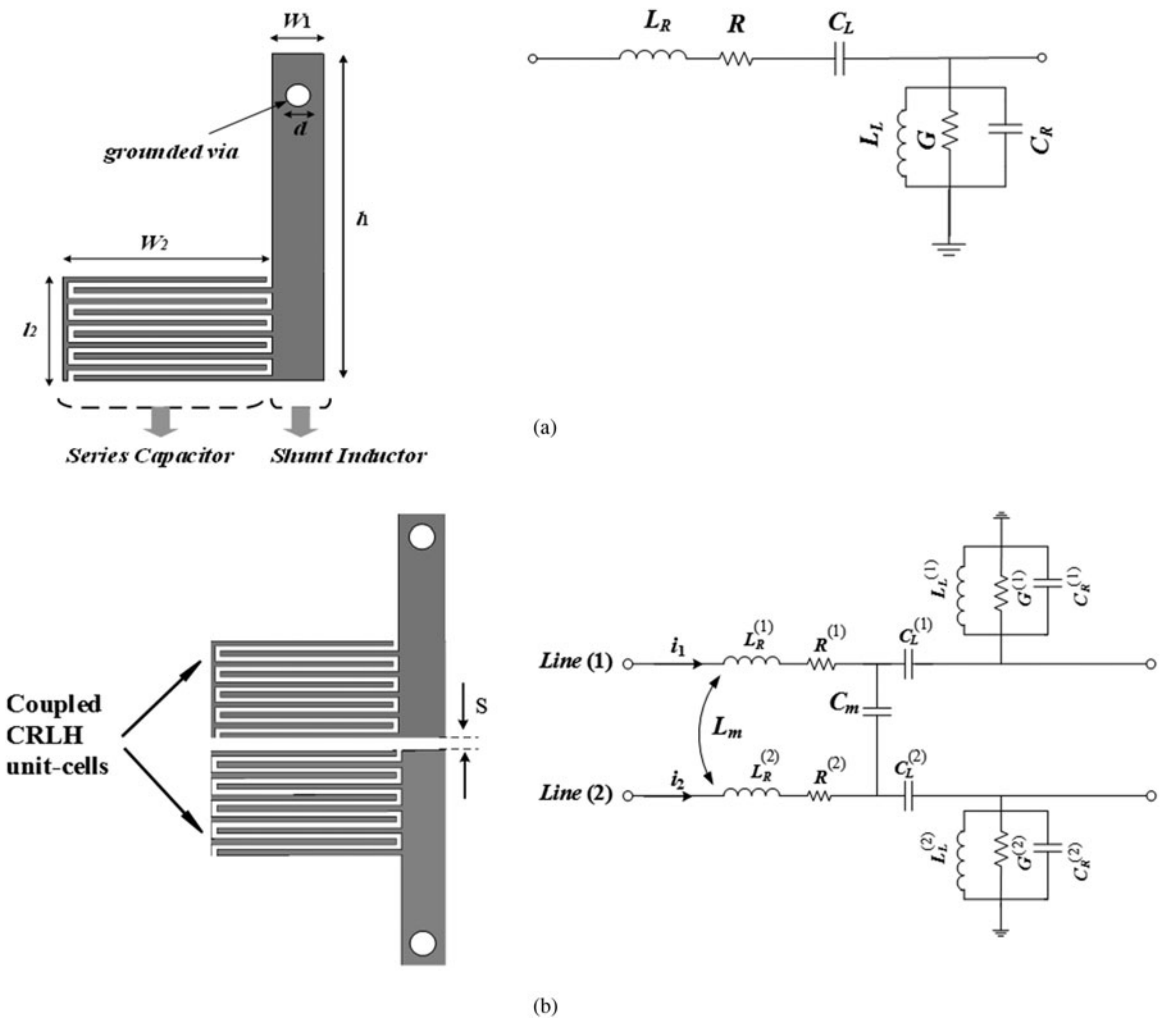

Fig. 2. (a) Layout of unit cell of fabricated coupler shown in Fig. 1(a), $l_1 = 8$ mm, $l_2 = 2.4$ mm, $w_1 = 1.1$ mm, $w_2 = 5$ mm, $d = 0.6$ mm, and its equivalent circuit model, and (b) the CRLH coupled unit cells and equivalent circuit model including the coupling capacitance C_m and mutual inductance L_m.

Discretized equations using the CN-FDTD method

This section is devoted to discretized coupled differential equations based on the CN-FDTD method. By first considering a single CRLH TL, generalization of the MCTL equations can be fairly straightforward. As shown in Fig. 3, a voltage source v_s is applied to the input of a CRLH TL, which is terminated by resistive impedances R_s and R_l. The CRLH TL is divided into N nodal currents and voltages along the line. The governing Telegrapher's equation to a single-conductor CRLH TL is stated as:

$$\begin{cases} \dfrac{\partial v}{\partial x} + R\,i + L_R\dfrac{\partial i}{\partial t} + \dfrac{v_{C_L}}{\Delta x} = 0 \\ \dfrac{C_L}{\Delta x}\dfrac{\partial v_{C_L}}{\partial t} - i = 0 \\ \dfrac{\partial i}{\partial x} + G v + C_R\dfrac{\partial v}{\partial t} + \dfrac{i_{L_L}}{\Delta x} = 0 \\ \dfrac{L_L}{\Delta x}\dfrac{\partial i_{L_L}}{\partial t} - v = 0 \end{cases}, \tag{6}$$

which becomes:

$$\begin{cases} L_R(i^{n+1}_{k+1/2} - i^{n}_{k+1/2}) + \dfrac{\Delta t}{2}R(i^{n+1}_{k+1/2} + i^{n}_{k+1/2}) + \dfrac{r}{2}(v^{n+1}_{k+1} - v^{n+1}_{k}) \\ \quad + \dfrac{r}{2}(v^{n}_{k+1} - v^{n}_{k}) + \dfrac{r}{2}({v_{C_L}}^{n+1}_{k+1/2} + {v_{C_L}}^{n}_{k+1/2}) = 0 \\ \dfrac{C_L}{\Delta x}({v_{C_L}}^{n+1}_{k+1/2} - {v_{C_L}}^{n}_{k+1/2}) - \dfrac{\Delta t}{2}(i^{n+1}_{k+1/2} + i^{n}_{k+1/2}) = 0 \\ C_R(v^{n+1}_{k} - v^{n}_{k}) + \dfrac{\Delta t}{2}G(v^{n+1}_{k} + v^{n}_{k}) + \dfrac{r}{2}(i^{n+1}_{k+1/2} - i^{n+1}_{k-1/2}) \\ \quad + \dfrac{r}{2}(i^{n}_{k+1/2} - i^{n}_{k-1/2}) + \dfrac{r}{2}({i_{L_L}}^{n+1}_{k} + {i_{L_L}}^{n}_{k}) = 0 \\ \dfrac{L_L}{\Delta x}({i_{L_L}}^{n+1}_{k} - {i_{L_L}}^{n}_{k}) - \dfrac{\Delta t}{2}(v^{n+1}_{k} + v^{n}_{k}) = 0 \end{cases}, \tag{7}$$

where $r = \Delta t/\Delta x$ and k denotes the position index as shown in Fig. 3 and n represents the nth time step size Δt. Generalizing to a MCTL consisting of two coupled CRLH TLs results in a total number of $2 \times 4N$ unknowns, which can be denoted by the

https://doi.org/10.1017/S1759078718001393 Published online by Cambridge University Press

vector $\mathbf{U} = [\mathbf{u}_v^T\ \mathbf{u}_i^T\ \mathbf{u}_{v_{C_L}}^T\ \mathbf{u}_{i_{L_L}}^T]^T$ with:

$$\begin{cases} \mathbf{u}_v^T = [v_1^1 \dots v_1^N \ \vdots \ v_2^1 \dots v_2^N], \quad \mathbf{u}_i^T = [i_1^1 \ \dots \ i_1^N \ \vdots \ i_2^1 \ \dots \ i_2^N] \\ \mathbf{u}_{v_{C_L}}^T = [v_{C_L^{(1)}}^1 \dots v_{C_L^{(1)}}^N \ \vdots \ v_{C_L^{(2)}}^1 \dots v_{C_L^{(2)}}^N], \\ \mathbf{u}_{i_{L_L}}^T = [i_{L_L^{(1)}}^1 \ \dots \ i_{L_L^{(1)}}^N \ \vdots \ i_{L_L^{(2)}}^1 \ \dots \ i_{L_L^{(2)}}^N] \end{cases} \tag{8}$$

and the superscript N represents the number of the line sections. The discretized matrix of the CRLH coupled-line coupler by applying the CN method to (3), (4) can be expressed as:

$$\mathbf{N}_L \mathbf{U}^{n+1} = \mathbf{N}_R \mathbf{U}^n, \tag{9}$$

with

$$\mathbf{N}_L = \begin{bmatrix} \frac{r}{2}(\mathbf{I}_N^+ - \mathbf{I}_N) \otimes \mathbf{I}_2 & \mathbf{I}_N \otimes \left(\mathbf{L}_R + \frac{\Delta t}{2}\mathbf{R}\right) & \left(\frac{r}{2}\right)\mathbf{I}_N \otimes \mathbf{I}_2 & \mathbf{I}_N \otimes 0_{2\times 2} \\ \mathbf{I}_N \otimes 0_{2\times 2} & \left(\frac{\Delta t}{2}\right)\mathbf{I}_N \otimes \mathbf{I}_2 & \left(\frac{-\mathbf{C}_L}{\Delta x}\right)\mathbf{I}_N \otimes \mathbf{I}_2 & \mathbf{I}_N \otimes 0_{2\times 2} \\ \mathbf{I}_N \otimes \left(\mathbf{C}_R + \frac{\Delta t}{2}\mathbf{G}\right) & \frac{r}{2}(\mathbf{I}_N - \mathbf{I}_N^-) \otimes \mathbf{I}_2 & \mathbf{I}_N \otimes 0_{2\times 2} & \left(\frac{r}{2}\right)\mathbf{I}_N \otimes \mathbf{I}_2 \\ \left(\frac{\Delta t}{2}\right)\mathbf{I}_N \otimes \mathbf{I}_2 & \mathbf{I}_N \otimes 0_{2\times 2} & \mathbf{I}_N \otimes 0_{2\times 2} & \left(\frac{-\mathbf{L}_L}{\Delta x}\right)\mathbf{I}_N \otimes \mathbf{I}_2 \end{bmatrix}, \tag{10}$$

$$\mathbf{N}_R = \begin{bmatrix} \frac{r}{2}(\mathbf{I}_N - \mathbf{I}_N^+) \otimes \mathbf{I}_2 & \mathbf{I}_N \otimes \left(\mathbf{L}_R - \frac{\Delta t}{2}\mathbf{R}\right) & \left(\frac{-r}{2}\right)\mathbf{I}_N \otimes \mathbf{I}_2 & \mathbf{I}_N \otimes 0_{2\times 2} \\ \mathbf{I}_N \otimes 0_{2\times 2} & \left(\frac{-\Delta t}{2}\right)\mathbf{I}_N \otimes \mathbf{I}_2 & \left(\frac{-\mathbf{C}_L}{\Delta x}\right)\mathbf{I}_N \otimes \mathbf{I}_2 & \mathbf{I}_N \otimes 0_{2\times 2} \\ \mathbf{I}_N \otimes \left(\mathbf{C}_R - \frac{\Delta t}{2}\mathbf{G}\right) & \frac{r}{2}(\mathbf{I}_N^- - \mathbf{I}_N) \otimes \mathbf{I}_2 & \mathbf{I}_N \otimes 0_{2\times 2} & \left(\frac{-r}{2}\right)\mathbf{I}_N \otimes \mathbf{I}_2 \\ \left(\frac{-\Delta t}{2}\right)\mathbf{I}_N \otimes \mathbf{I}_2 & \mathbf{I}_N \otimes 0_{2\times 2} & \mathbf{I}_N \otimes 0_{2\times 2} & \left(\frac{-\mathbf{L}_L}{\Delta x}\right)\mathbf{I}_N \otimes \mathbf{I}_2 \end{bmatrix}, \tag{11}$$

wherein

$$\mathbf{I}_N = \begin{bmatrix} 1 & 0 & 0 & \cdots \\ 0 & 1 & 0 & \ddots \\ 0 & 0 & 1 & \ddots \\ \vdots & \ddots & \ddots & \ddots \end{bmatrix}_{N\times N} \quad \mathbf{I}_N^+ = \begin{bmatrix} 0 & 1 & 0 & \cdots \\ 0 & 0 & 1 & \ddots \\ 0 & 0 & 0 & \ddots \\ \vdots & \ddots & \ddots & \ddots \end{bmatrix}_{N\times N}, \quad \mathbf{I}_N^- = \begin{bmatrix} 0 & 0 & 0 & \cdots \\ 1 & 0 & 0 & \ddots \\ 0 & 1 & 0 & \ddots \\ \vdots & \ddots & \ddots & \ddots \end{bmatrix}_{N\times N}, \tag{12}$$

and "⊗" stands for the *matrix Kronecker* product [39].

Boundary conditions

Boundary condition (BC) is first introduced in the same way as a single-conductor TL and then generalized to a MCTL. As demonstrated in Fig. 3, v_{in}, v_L, i_s, and i_L correspond to the voltages and currents at line input and load, respectively. By selecting the first equation in (7), BC is imposed at load for $k = (N - 1/2)$ leading to [40]:

$$L_R(i_N^{n+1} - i_N^n) + \frac{\Delta t}{2}R(i_N^{n+1} + i_N^n) + \frac{r}{2}(v_{N+1/2}^{n+1} - v_{N-1/2}^{n+1}) + \frac{r}{2}(v_{N+1/2}^n - v_{N-1/2}^n) + \frac{r}{2}({v_{C_L}}_N^{n+1} + {v_{C_L}}_N^n) = 0, \tag{13}$$

by replacing $v_L = R_L i_L$ and accordingly $v_N = R_L i_{N-1}$, after a simple rearrangement, the above equation becomes:

$$\left[-\frac{r}{2}v_{N-1} + \frac{r}{2}(v_{C_L})_N + \left(L_R + \frac{\Delta t}{2}R + \frac{r}{2}R_L\right)i_N\right]^{(n+1)} = \left[+\frac{r}{2}v_{N-1} - \frac{r}{2}(v_{C_L})_N + \left(L_R - \frac{\Delta t}{2}R - \frac{r}{2}R_L\right)i_N\right]^{(n)}, \tag{14}$$

where subscripts are associated with the array indices.

Similarly, the first equation in (7) for $k = 1$ at source, leads to:

$$L_R(i_{3/2}^{n+1} - i_{3/2}^n)\frac{\Delta t}{2}R(i_{3/2}^{n+1} + i_{3/2}^n) + \frac{r}{2}(v_2^{n+1} - v_1^{n+1}) + \frac{r}{2}(v_2^n - v_1^n) + \frac{r}{2}({v_{C_L}}_{3/2}^{n+1} + {v_{C_L}}_{3/2}^n) = 0, \tag{15}$$

for $-v_S + R_S i_S + v_{in} = 0$ and replacing v_{in} by v_1 and i_S by i_1,

https://doi.org/10.1017/S1759078718001393 Published online by Cambridge University Press

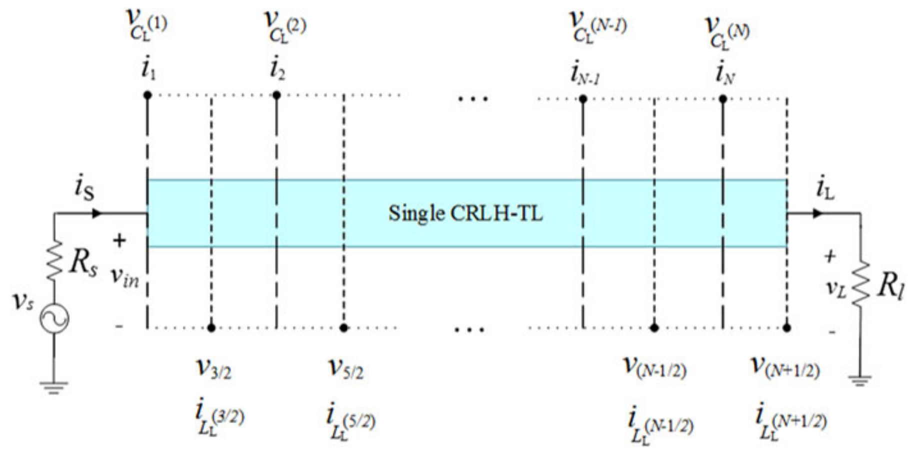

Fig. 3. Discretization of a single-conductor CRLH TL driven by a voltage source.

becomes:

$$\left[\frac{r}{2}v_2+\frac{r}{2}(v_{C_L})_1+\left(L_R+\frac{\Delta t}{2}R+\frac{r}{2}R_S\right)i_1\right]^{(n+1)} \cong \left[-\frac{r}{2}v_2-\frac{r}{2}(v_{C_L})_1+\left(L_R-\frac{\Delta t}{2}R-\frac{r}{2}R_S\right)i_1\right]^{(n)}+rv_S^n. \quad (16)$$

To generalize the corresponding BCs to a coupled-line coupler, let the first and second lines be, respectively, terminated by $R_S^{(1)}$ and $R_S^{(2)}$ at the source and by $R_L^{(1)}$ and $R_L^{(2)}$ at the load. Thus, $\mathbf{R}_S$ and $\mathbf{R}_L$ matrices defining the source and load impedance matrices, respectively, are:

$$\begin{cases}\mathbf{R}_S = diag(R_S^{(1)},\ R_S^{(2)})\\ \mathbf{R}_L = diag(R_L^{(1)},\ R_L^{(2)})\end{cases}. \quad (17)$$

Terminal BCs are imposed to the aforementioned coupler by modifying $\mathbf{N}_L$ and $\mathbf{N}_R$. BCs applied at load lead to:

$$\begin{cases}\mathbf{N}_L(2N-3:2N-2,:)=0\\ \mathbf{N}_L(2N-3:2N-2,2N-3:2N-2)=-\left(\frac{r}{2}\right)\mathbf{I}_2\\ \mathbf{N}_L(2N-3:2N-2,\ 4N-1:4N)=\mathbf{L}_R+\left(\frac{\Delta t}{2}\right)\mathbf{R}+\left(\frac{r}{2}\right)\mathbf{R}_L\\ \mathbf{N}_L(2N-3:2N-2,\ 6N-1:6N)=\left(\frac{r}{2}\right)\mathbf{I}_2\\ \mathbf{N}_R(2N-3:2N-2,:)=0\\ \mathbf{N}_R(2N-3:2N-2,2N-3:2N-2)=\left(\frac{r}{2}\right)\mathbf{I}_2\\ \mathbf{N}_R(2N-3:2N-2,\ 4N-1:4N)=\mathbf{L}_R-\left(\frac{\Delta t}{2}\right)\mathbf{R}-\left(\frac{r}{2}\right)\mathbf{R}_L\\ \mathbf{N}_R(2N-3:2N-2,\ 6N-1:6N)=-\left(\frac{r}{2}\right)\mathbf{I}_2\end{cases} \quad (18)$$

and the corresponding matrices for the source must be modified as follows:

$$\begin{cases}\mathbf{N}_L(1:2,:)=0\\ \mathbf{N}_L(1:2,3:4)=\left(\frac{r}{2}\right)\mathbf{I}_2\\ \mathbf{N}_L(1:2,\ 2N+1:2N+2)=\mathbf{L}_R+\left(\frac{\Delta t}{2}\right)\mathbf{R}+\left(\frac{r}{2}\right)\mathbf{R}_S\\ \mathbf{N}_L(1:2,\ 4N+1:4N+2)=\left(\frac{r}{2}\right)\mathbf{I}_2\\ \mathbf{N}_R(1:2,:)=0\\ \mathbf{N}_R(1:2,3:4)=-\left(\frac{r}{2}\right)\mathbf{I}_2\\ \mathbf{N}_R(1:2,\ 2N+1:2N+2)=\mathbf{L}_R-\left(\frac{\Delta t}{2}\right)\mathbf{R}-\left(\frac{r}{2}\right)\mathbf{R}_S\\ \mathbf{N}_R(1:2,\ 4N+1:4N+2)=-\left(\frac{r}{2}\right)\mathbf{I}_2\end{cases} \quad (19)$$

Finally, the time marching is conducted as:

$$\mathbf{N}_L\mathbf{U}^{n+1}=\mathbf{N}_R\mathbf{U}^n+r\mathbf{V}_S^n, \quad (20)$$

where the $\mathbf{V}_S^n$ is the input voltage vector at the nth time step.

Stability analysis

To ensure the stability issue of the CN-FDTD method, the associated amplification matrix ($\mathbf{Q}=\mathbf{N}_L^{-1}\mathbf{N}_R$) and the corresponding Eigen-equation ($\mathbf{N}_R\mathbf{u}=\lambda\mathbf{N}_L\mathbf{u}$), are derived when Δt approaches infinity [40]:

https://doi.org/10.1017/S1759078718001393 Published online by Cambridge University Press

$$\lambda \begin{bmatrix} \frac{1}{2\Delta x}(\mathbf{I}_N^+ - \mathbf{I}_N)\otimes \mathbf{I}_2 & \mathbf{I}_N \otimes \left(\frac{\mathbf{R}}{2}\right) & \left(\frac{1}{2\Delta x}\right)\mathbf{I}_N \otimes \mathbf{I}_2 & \mathbf{I}_N \otimes 0_{2\times 2} \\ \mathbf{I}_N \otimes 0_{2\times 2} & \left(\frac{1}{2}\right)\mathbf{I}_N \otimes \mathbf{I}_2 & \mathbf{I}_N \otimes 0_{2\times 2} & \mathbf{I}_N \otimes 0_{2\times 2} \\ \mathbf{I}_N \otimes \left(\frac{\mathbf{G}}{2}\right) & \frac{1}{2\Delta x}(\mathbf{I}_N - \mathbf{I}_N^-)\otimes \mathbf{I}_2 & \mathbf{I}_N \otimes 0_{2\times 2} & \left(\frac{1}{2\Delta x}\right)\mathbf{I}_N \otimes \mathbf{I}_2 \\ \left(\frac{1}{2}\right)\mathbf{I}_N \otimes \mathbf{I}_2 & \mathbf{I}_N \otimes 0_{2\times 2} & \mathbf{I}_N \otimes 0_{2\times 2} & \mathbf{I}_N \otimes 0_{2\times 2} \end{bmatrix} \mathbf{u}$$
$$= \begin{bmatrix} \frac{1}{2\Delta x}(\mathbf{I}_N - \mathbf{I}_N^+)\otimes \mathbf{I}_2 & \mathbf{I}_N \otimes \left(-\frac{\mathbf{R}}{2}\right) & \left(\frac{-1}{2\Delta x}\right)\mathbf{I}_N \otimes \mathbf{I}_2 & \mathbf{I}_N \otimes 0_{2\times 2} \\ \mathbf{I}_N \otimes 0_{2\times 2} & \left(\frac{-1}{2}\right)\mathbf{I}_N \otimes \mathbf{I}_2 & \mathbf{I}_N \otimes 0_{2\times 2} & \mathbf{I}_N \otimes 0_{2\times 2} \\ \mathbf{I}_N \otimes \left(-\frac{\mathbf{G}}{2}\right) & \frac{1}{2\Delta x}(\mathbf{I}_N^- - \mathbf{I}_N)\otimes \mathbf{I}_2 & \mathbf{I}_N \otimes 0_{2\times 2} & \left(\frac{-1}{2\Delta x}\right)\mathbf{I}_N \otimes \mathbf{I}_2 \\ \left(\frac{-1}{2}\right)\mathbf{I}_N \otimes \mathbf{I}_2 & \mathbf{I}_N \otimes 0_{2\times 2} & \mathbf{I}_N \otimes 0_{2\times 2} & \mathbf{I}_N \otimes 0_{2\times 2} \end{bmatrix} \mathbf{u}, \quad (21)$$

and as $\Delta t \to \infty$, it finally further simplifies to:

$$(1+\lambda)\,\mathbf{u} = 0, \quad (22)$$

which satisfies the unit spectral radius, i.e., the unconditional stability of the CN-FDTD method is warranted [29]. The stability results are numerically validated later for the specific fabricated coupler.

Extraction of the unit-cell parameters

In order to extract unit-cell parameters, first the scattering parameters of the corresponding series capacitance and shunt inductance structures are computed separately by either full-wave analysis or measurements. Then the *S*-parameters are converted to the corresponding *Z*-parameters or *Y*-parameters [14]. Finally, the LC parameters are retrieved according to standard derivations with respect to the extraction frequency [41]. According to Fig. 1, this CRLH coupler, fabricated on the Rogers RT/Duroid 5880 substrate with dielectric constant $\varepsilon_r = 2.2$ and thickness of $h = 1.27$ mm, contains nine unit cells with each having a length of 6.1 mm, assumed to be lossless ($R^{(1)} = R^{(2)} = G^{(1)} = G^{(2)} = 0$). The extracted lumped circuit parameters of each unit cell are reported in Table 1.

Results and discussion

Accuracy

In this section, the accuracy of the CN-FDTD method applied to the CRLH coupled-line coupler is investigated and compared with the LF-FDTD method. A sinusoidal excitation oscillating at 3.9 GHz is connected to the input port and the outputs are measured from the through and the coupled ports of the coupler.

As mentioned before, there is a trade-off between CPU time and accuracy of the CN-FDTD method. Here, for $10 \times \Delta t_{max}$ ($\Delta t_{max} = 1.8$ ps which is the maximum time step size corresponding to the LF scheme), the accuracy is well maintained, and by increasing the time step size, the accuracy is degraded as shown in Fig. 4.

In order to mathematically assess this dependency between the computation cost and accuracy, the relative error (denoted by r_e) computed by the CN and LF schemes is reported in Table 2, wherein:

$$r_e = \frac{\sqrt{\sum_i |V_o^{\Delta t}(i\Delta t) - V_o^{\Delta t\,\max}(i\Delta t)|^2}}{\sqrt{\sum_i |V_o^{\Delta t\,\max}(i\Delta t)|^2}}, \quad (23)$$

where $V_o^{\Delta t\,\max}$ and $V_o^{\Delta t}$ represent load voltages at the end of either through or coupled ports for Δt_{max} and Δt voltage values, respectively [43].

According to Table 2, the time step size of $10\Delta t_{max}$ is considered to be the threshold of optimum accuracy with a negligible error value, and that beyond this point, the response becomes erroneous noticeably. Therefore, a clear trade-off is observed between CPU time and desired accuracy.

Time gain

The time gain, as the relative CPU time of the LF-FDTD compared with the CN-FDTD method (T_{LF}/T_{CN}), versus different temporal step size at 3.9 and 6 GHz is reported in Table 3.

As it is evident, the CN method requires much less CPU time compared with the LF method as no constraint is imposed on temporal step size until the accuracy level is satisfied. In this study, for $\Delta t = 10\Delta t_{max}$, the time gain accompanied to a satisfactory accuracy is achieved.

Stability

To examine the stability, the spectral radius of the amplification matrix for the LF- and CN-FDTD methods is computed for a range of Δt and reported in Fig. 5. In the LF scheme restrained by the CFL number, the spectral radius rises unboundedly once

Table 1. Extracted values of the CRLH coupled-line unit cell [42]

Lumped model parameters	Numerical values
$L_R^{(1)} = L_R^{(2)}$	2.45 nH
$C_R^{(1)} = C_R^{(2)}$	0.5 pF
$L_L^{(1)} = L_L^{(2)}$	3.38 nH
$C_L^{(1)} = C_L^{(2)}$	0.68 pF
L_m	1 nH
C_m	0.4 pF

Table 2. Estimated error (r_e) versus Δt

Temporal step size (Δt)	r_e for through port (%)	r_e for coupled port (%)
$10\Delta t_{max}$	4.14	3.65
$11\Delta t_{max}$	15.12	14.35
$12\Delta t_{max}$	26.5	18.11
$13\Delta t_{max}$	31.41	24.81
$14\Delta t_{max}$	44.12	30.34

Table 3. Time gain of the CN method for different time step sizes

Temporal step size	Time gain at 3.9 GHz	Time gain at 6 GHz
Δt_{max}	0.42	0.29
$2\Delta t_{max}$	0.85	0.59
$4\Delta t_{max}$	1.7	1.23
$6\Delta t_{max}$	2.55	1.85
$8\Delta t_{max}$	3.44	2.8
$10\Delta t_{max}$	4.68	3.65
$11\Delta t_{max}$	4.72	3.9
$13\Delta t_{max}$	5.56	4.81
$14\Delta t_{max}$	6.42	5.34

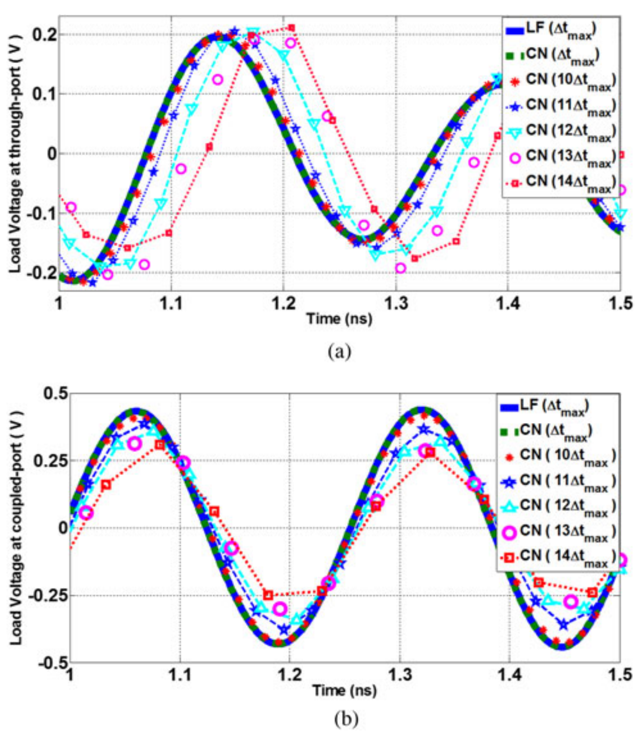

Fig. 4. The voltage at the end of (a) through port, (b) coupled port corresponding to the LF at Δt_{max} and CN at Δt_{max} and the CN at $k \times \Delta t_{max}$ (k varies from 10 to 14).

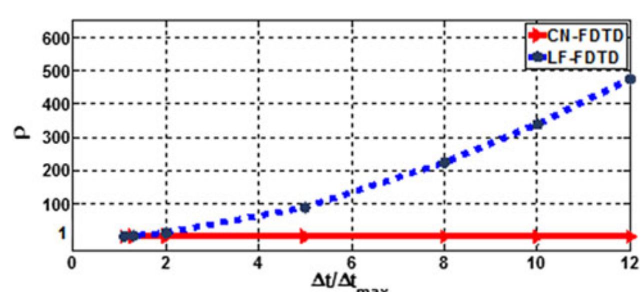

Fig. 5. The spectral radius analysis versus time step size.

Δt becomes greater than $\Delta t_{max} = 1.8$ ps at 3.9 GHz. Thus, the LF method becomes unstable, though the spectral radius of the CN method is equal to unity.

Scattering parameters

The scattering parameters (S-parameters) can be extracted from the time-domain results [40]. It is conducted by first computing the corresponding Z-parameters according to:

$$Z_{ij}(f) = \left[\frac{V_i(f)}{I_j(f)}\right]\Bigg|_{I_k=0,\ k\neq j}, \tag{24}$$

where subscripts i and j stand for the port numbers. In this approach, Z_{ii} and Z_{ji} are computed by applying a proper Gaussian excitation pulse to the beginning of the port i, while port j is open-circuited. Similarly, Z_{ij} and Z_{jj} are extracted by applying the excitation signal to port j and open-circuiting port i. Then the S-parameters are retrieved as [14]:

$$\mathbf{S} = (\mathbf{Z} + Z_0\mathrm{I})^{-1}(\mathbf{Z} - Z_0\mathrm{I}). \tag{25}$$

The coupled-line coupler as a four-port device is excited by a Gaussian pulse with peak time and spread of 80 and 20 ps, respectively, at the input port and the outputs are extracted from the through and coupled ports while matched to Z_0 (50 Ω resistor). There is a backward-wave coupling from approximately 3.2–4.5 GHz and also the through coupling ranging from 1.5 to 3.1 GHz, showing a dual-band operation. As illustrated in Fig. 6, the S-parameter results extracted from both LF- and CN-FDTD methods are in good agreement with the measurement results.

https://doi.org/10.1017/S1759078718001393 Published online by Cambridge University Press

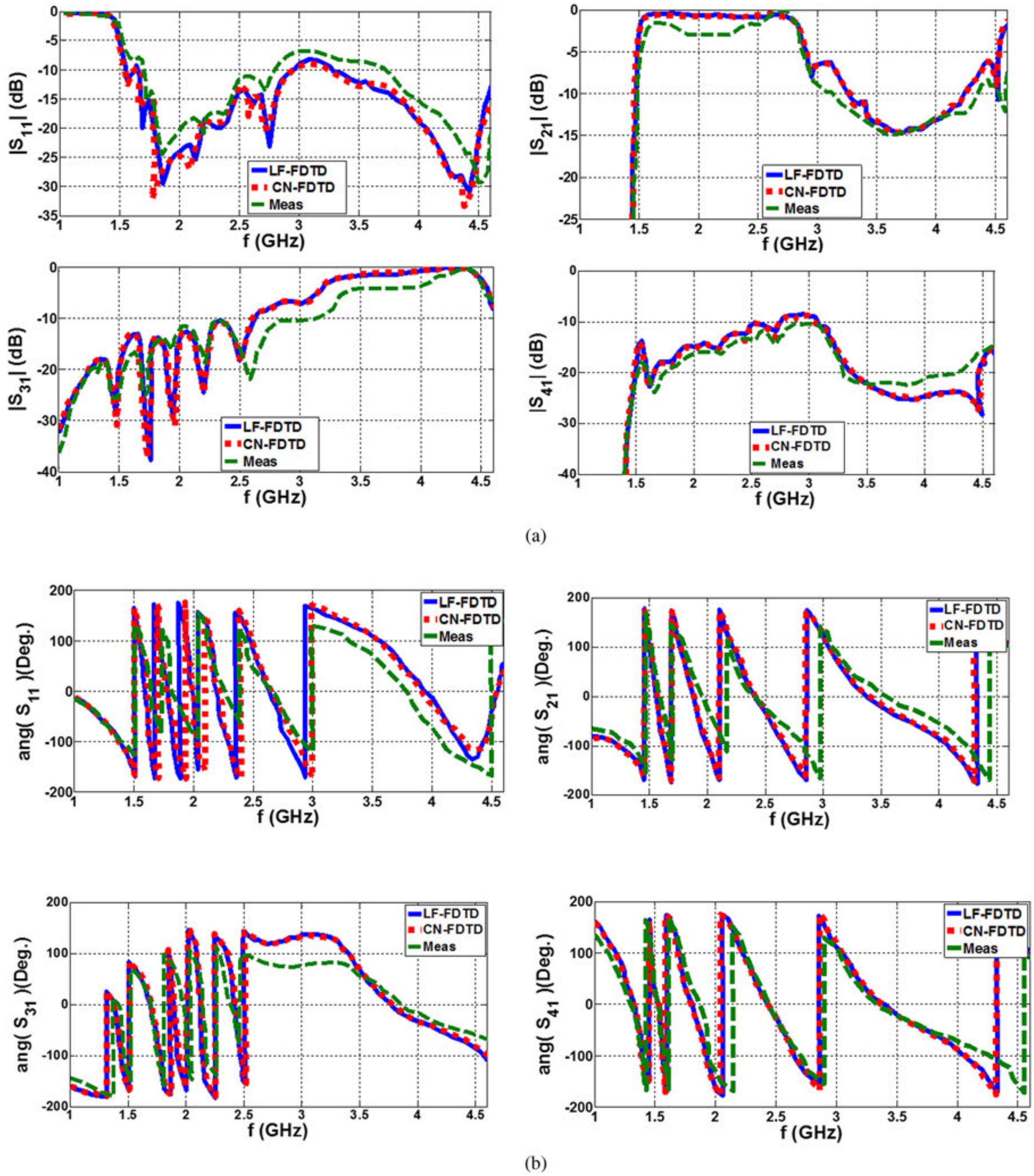

Fig. 6. *S*-parameters of the CRLH coupled-line coupler shown in Fig. 1. (a) Magnitude and (b) phase.

Conclusion

In this paper, the CN-FDTD was successfully used to analyze a CRLH coupled-line coupler. Unconditional stability of this method has been confirmed. The accuracy of the CN has been verified by comparison of the results from CN to LF scheme and also the measurements. It is concluded that the CN-FDTD method has improved the time gain with satisfying accuracy level, whilst the temporal step size increased up to 10 times.

Author ORCIDs. Mahdieh Gholami Mayani http://orcid.org/0000-0002-4301-5734.

References

1. **Viktor GV** (1968) The electrodynamics of substances with simultaneously negative values of ϵ AND μ. *Soviet Physics-Uspekhi* **10**, 509.
2. **Pendry JB, Holden AJ, Robbins DJ and Stewart WJ** (1999) Magnetism from conductors and enhanced nonlinear phenomena. *IEEE Transactions on Microwave Theory and Techniques* **47**, 2075–2084.
3. **Zhu C, Liang C-H and Li L** (2011) Broadband negative index metamaterials with low-loss. AEU – *International Journal of Electronics and Communications* **65**, 724–727.
4. **Oliner AA** (2003) A planar negative-refractive-index medium without resonant elements. *IEEE MTT-S International Microwave Symposium Digest*, USA.

https://doi.org/10.1017/S1759078718001393 Published online by Cambridge University Press

5. **Iyer AK and Eleftheriades GV** (2002) Negative refractive index metamaterials supporting 2-D waves. *2002 IEEE MTT-S International Microwave Symposium Digest (Cat. No.02CH37278)*, Washington.
6. **Caloz C and Itoh T** (2004) Transmission line approach of left-handed (LH) materials and microstrip implementation of an artificial LH transmission line. *IEEE Transactions on Antennas and Propagation* **52**, 1159–1166.
7. **Afrooz K, Abdipour A and Martin F** (2012) Time domain analysis of one-dimensional linear and non-linear composite right/left-handed transmission lines using finite-difference time-domain method. *IET Microwaves, Antennas* and Propagation **6**, 312–325.
8. **Lai A, Itoh T and Caloz C** (2004) Composite right/left-handed transmission line metamaterials. *IEEE Microwave Magazine* **5**, 34–50.
9. **Lei L, Caloz C and Itoh T** (2002) Dominant mode leaky-wave antenna with backfire-to-endfire scanning capability. *Electronics Letters* **38**, 1414–1416.
10. **Antoniades MA and Eleftheriades GV** (2003) Compact linear lead/lag metamaterial phase shifters for broadband applications. *IEEE Antennas and Wireless Propagation Letters* **2**, 103–106.
11. **Caloz C, Sanada A and Itoh T** (2004) A novel composite right-/left-handed coupled-line directional coupler with arbitrary coupling level and broad bandwidth. *IEEE Transactions on Microwave Theory and Techniques* **52**, 980–992.
12. **Danaeian M, Afrooz K and Hakimi A** (2018) Miniaturization of substrate integrated waveguide filters using novel compact metamaterial unit-cells based on SIR technique. *AEU – International Journal of Electronics and Communications* **84**, 62–73.
13. **Mongia R, Bhartia P, Bahl I and Hong J** (1999) *RF and Microwave Coupled-Line Circuits*. Norwood, MA: Artech House.
14. **Pozar D** (1998) *Microwave Engineering*. New York: Wiley.
15. **Lange J** (1969) Interdigitated stripline quadrature hybrid (correspondence). *IEEE Transactions on Microwave Theory and Techniques* **17**, 1150–1151.
16. **Keshavarz R, Movahhedi M and Abdipour A** (2012) A broadband and compact asymmetrical backward coupled-line coupler with high coupling level. *AEU – International Journal of Electronics and Communications* **66**, 569–574.
17. **Hussein YA and El-Ghazaly SM** (2004) Modeling and optimization of microwave devices and circuits using genetic algorithms. *IEEE Transactions on Microwave Theory and Techniques* **52**, 329–336.
18. **Movahhedi M and Abdipour A** (2005) Accelerating the transient simulation of semiconductor devices using filter-bank transforms. in *European Gallium Arsenide and Other Semiconductor Application Symposium, GAAS*, Paris.
19. **Mirzavand R, Abdipour A, Moradi G and Movahhedi M** (2010) Full-wave semiconductor devices simulation using adi-FDTD method. *Progress In Electromagnetics Research M* **11**, 191–202.
20. **Mirzavand R, Abdipour A, Moradi G and Movahhedi M** (2011) Full-wave semiconductor devices simulation using meshless and finite-difference time-domain approaches. *IET Microwaves, Antennas* and Propagation **5**, 685–691.
21. **Zhang Y and Spielman BE** (2007) A stability analysis for time-domain method-of-moments analysis of 1-D double-negative transmission lines. *IEEE Transactions on Microwave Theory and Techniques on* **55**, 1887–1898.
22. **Gomez-Diaz JS, Gupta S, Alvarez-Melcon A and Caloz C** (2009) Investigation on the phenomenology of impulse-regime metamaterial transmission lines. *IEEE Transactions on Antennas and Propagation* **57**, 4010–4014.
23. **Gomez-Diaz JS, Gupta S, Lvarez-melcon AA and Caloz C** (2010) Efficient time-domain analysis of highly dispersive linear and non-linear metamaterial waveguide and antenna structures operated in the impulse-regime. *IET Microwaves, Antennas and Propagation* **4**, 1617–1625.
24. **Ghadimi A and Asadi S** (2018) Modelling of composite right/left-handed active multiconductor transmission lines (AMCTL) in time domain. *International Journal of Numerical Modelling* **31**, e2257.
25. **Taflove A** (1995) *Computational Electrodynamics: The Finite-Difference Time-Domain Method*. Norwood, MA: Artech House.
26. **Thomas J** (1998) *Numerical Partial Differential Equations: Finite Difference Methods*. New York: Springer-Verlag.
27. **Guilin S and Trueman CW** (2006) Efficient implementations of the Crank-Nicolson scheme for the finite-difference time-domain method. *IEEE Transactions on Microwave Theory and Techniques* **54**, 2275–2284.
28. **Yang Y, Chen RS, Wang DX and Yung EKN** (2007) Unconditionally stable Crank-Nicolson finite-different time-domain method for simulation of three-dimensional microwave circuits. *IET Microwaves, Antennas and Propagation* **1**, 937–942.
29. **Honarbakhsh B and Asadi S** (2017) Analysis of multiconductor transmission lines using the CN-FDTD method. *IEEE Transactions on Electromagnetic Compatibility* **59**, 184–192.
30. **Namiki T** (1999) A new FDTD algorithm based on alternating-direction implicit method. *IEEE Transactions on Microwave Theory and Techniques* **47**, 2003–2007.
31. **Fenghua Z, Zhizhang C and Jiazong Z** (2000) Toward the development of a three-dimensional unconditionally stable finite-difference time-domain method. *IEEE Transactions on Microwave Theory and Techniques* **48**, 1550–1558.
32. **Garcia SG, Tae-Woo L and Hagness SC** (2002) On the accuracy of the ADI-FDTD method. *IEEE Antennas and Wireless Propagation Letters* **1**, 31–34.
33. **Lee J and Fornberg B** (2004) Some unconditionally stable time stepping methods for the 3D Maxwell's equations. *Journal of Computational and Applied Mathematics* **166**, 497–523.
34. **Shibayama J, Muraki M, Yamauchi J and Nakano H** (2005) Efficient implicit FDTD algorithm based on locally one-dimensional scheme. *Electronics Letters* **41**, 1046–1047.
35. **Liu QF, Chen Z and Yin WY** (2009) An arbitrary-order LOD-FDTD method and its stability and numerical dispersion. *IEEE Transactions on Antennas and Propagation* **57**, 2409–2417.
36. **Kijun L, Song Jae L, Dong Chul P and Yeon Choon C** (1997) Equivalent circuit model for the time-domain analysis of multiconductor transmission lines by the implicit FDTD method. in *IEEE 1997, EMC, Austin Style. IEEE 1997 International Symposium on Electromagnetic Compatibility. Symposium Record (Cat. No.97CH36113)*.
37. **Afrooz K and Abdipour A** (2012) Efficient method for time-domain analysis of lossy nonuniform multiconductor transmission line driven by a modulated signal using FDTD technique. *IEEE Transactions on Electromagnetic Compatibility* **54**, 482–494.
38. **Afrooz K** (2016) Unconditionally stable finite-difference time-domain algorithm for analysing composite right-/left-handed transmission line. *IET Microwaves, Antennas and Propagation* **10**, 339–346.
39. **Shi WS and Shi TK** (1997) *Matrix Calculus and Kroneker Product with Applications and C++ Programs*. USA: World Scientific Pub.
40. **Asadi S and Honarbakhsh B** (2017) Linear analysis of high-frequency field-effect transistors using the CN-FDTD method. *IEEE Transactions on Microwave Theory and Techniques* **65**, 1946–1954.
41. **Kantartzis NV and Tsiboukis TD** (2008) *Modern EMC analysis techniques*, vol. **1**. US: Morgan and Claypool Publishers.
42. **Caloz C and Itoh T** (2006) *Electromagnetic Metamaterials: Transmission Line Theory and Microwave Applications*. US: Wiley and IEEE Press.
43. **Gholami Mayani M and Asadi S** (2018) Analysis of dual-gate high electron mobility transistor using an unconditionally stable time domain method. *IET Science, Measurement and Technology* **12**, 698–705.

Mahdieh Gholami Mayani was born in Iran, in 1985. She received her B.S. from Shahrood University of Technology and M.S. degree in electrical engineering from Shahid Beheshti University of Tehran, respectively, in 2007 and 2016. She is currently research assistant in the Department of Electrical Engineering at the Shahid Beheshti University. Her research interests are numerical electromagnetics, Metamaterials, passive and active devices and multiconductor transmission lines.

Shahrooz Asadi received the B.Sc. degree in Electrical Engineering and the M.Sc. degree in Electronics both from Amirkabir University of Technology (Tehran Polytechnic), in 2003 and 2007, respectively and the Ph.D. degree in Electronics in the School of Information Technology and Engineering (SITE), University of Ottawa, Ottawa, ON, Canada. He joined Shahid Beheshti University in 2011 where he is an assistant professor. His research interests include linear and nonlinear time-domain modeling of millimeter-wave transistors, RF design of active and passive devices, design and optimization of solid state devices and multiconductor transmission lines and printed circuit board.

Dr Shokrollah Karimian is an Assistant Professor in School of Electrical Engineering at Shahid Beheshti University. As a member of IEEE, with over 50 publications, he has made valuable contribution to the RF and microwave/mm-wave community.

https://doi.org/10.1017/S1759078718001393 Published online by Cambridge University Press